厚生労働科学研究委託費

難治性疾患実用化研究事業

健康寿命の延伸、重症化遅延を目指した早老症治療薬の創出

平成２６年度　委託業務成果報告書

業務主任者　宮田　敏男

平成２７（２０１５）年　３月

別添１

厚生労働科学研究委託費

難治性疾患実用化研究事業

健康寿命の延伸、重症化遅延を目指した早老症治療薬の開発

平成２６年度　委託業務成果報告書

業務主任者　宮田　敏男

平成２７（2015）年　3月

別添２

目　　次

別添３

厚生労働科学研究委託費（難治性疾患実用化研究事業）
委託業務成果報告（総括・業務項目）

健康寿命の延伸、重症化遅延を目指した早老症治療薬の開発

業務主任者　宮田　敏男　東北大学大学院医学系研究科

研究要旨

日本人に多いウェルナー症候群（WRN）の原因は、RecQ型DNAヘリカーゼの変異と考えられているが、この変異が何故、早老症状をもたらすかは未解明であり、治療法はない。WRN患者の血中や繊維芽細胞で老化促進因子IGFBP-3と共にPAI-1が高発現しており、正常WRNがPAI-1発現を抑制していることが報告された。

申請者らは、早老症モデルのklothoマウスでPAI-1を欠損させると短命が著明に改善することや、血管老化モデルマウスにおいて、PAI-1欠損またはPAI-1阻害薬投与で、テロメアの短縮が抑制されることを発見した。PAI-1阻害薬は経口投与可能であり、同系列のPAI-1阻害薬が医師主導臨床試験に進んでいることから、臨床開発上の懸念は少ないと考えられる。本研究では、複数の早老症モデルマウスでの薬効の検証とメカニズム解析、およびPAI-1阻害薬の非臨床GLP試験の準備までを2年間で行う計画である。

klotho欠損マウスでの研究計画は、平成26年度でほぼ達成した。今後は早老症のみならず、老化に関連する諸疾患に対するPAI-1阻害薬の治療効果や作用機序の解析を行う予定である。

業務項目の担当責任者氏名・所属研究機関名及び所属研究機関における職名

宮田　敏男　東北大学大学院医学系研究科 教授

A. 研究目的

どの国も経験のない超高齢社会を迎えた我が国において、「健康寿命の延伸と健康格差の縮小」は喫緊の課題である。申請者らは、希少難治性疾患のウェルナー症候群をはじめ、老化に伴う組織機能の低下にPAI-1が関わり、PAI-1阻害薬により改善できる可能性を見出した。本研究では、経口PAI-1阻害薬の実用化を目指した非臨床GLP試験までに必要な研究を2年間で行う。

B. 研究方法

希少難治性疾患で日本人に多いウェルナー症候群の原因は、RecQ型DNAヘリカーゼ（WRN）の変異と考えられているが、この変異が何故、本疾患に特徴的な早老症状、糖尿病、動脈硬化、悪性腫瘍等をもたらすかは未解明であり、根本的治療法はまだない。PAI-1は、糖尿病、動脈硬化や悪性腫瘍のリスク因子であるばかりではなく、ウェルナー症候群患者の血中や繊維芽細胞で老化促進因子IGFBP-3と共に高発現し、正常WRNがPAI-1発現を抑制していることが報告された。申請者らは、早老症モデルのklothoマウスでPAI-1を欠損させると、短命、低身長が著明に改善することや、血管老化モデルマウスにおいて、PAI-1欠損またはPAI-1阻害薬（TM5441/5484）投与で、高血圧と動脈硬化が寛解し、テロメアの短縮がPAI-1阻害薬投与により抑制されることを発見した。TM5441/5484は、経口投与可能であり、同系列のPAI-1阻害薬が医師主導臨床試験に進んでおり、また安全性予備試験（非GLP）でも問題がないことから、安全性や製剤化における懸念は少なく、治療応用は比較的短期で可能と考えられる。本研究では、平成26年度は非臨床動物実験モデルにおける複数の早老症モデルマウスでの薬効の検証、平成27年度は薬効薬理研究による薬効発揮のメカニズム解析と非臨床GLP試験の準備までを行う。

日本は高齢化が世界的に最も早く進行している国であり、(1) 健康寿命の延伸と健康格差の縮小、(2) 生活習慣病の発症予防と重症化予防が出来る薬剤の開発が切望されている。ウェルナー症候群の臨床像はそれら課題の縮図と言って過言ではない。本研究において、PAI-1阻害薬の開発が成功すれば、一剤でウェルナー症候群の多様な老化病態に対して多面的な治療効果が期待できるばかりではなく、我が国が抱える生活習慣病の発症予防・重症化予防に効果を発揮する可能性が考えられ、画期的な治療薬の創出が期待できる。

本研究ではさらに、日本およびアメリカにおいてPAI-1の遺伝子多型を調べ老化マーカーとの相関を調べる予定であり、これらの知見を合わせることにより、PAI-1を標的とした老化関連の種々の病態に対する個別化医療の実現が期待される。

平成２６年度における研究開発計画項目、マイルストーン及び研究開発方法

達成目標：早老症マウスモデルにおけるPAI-1阻害薬の薬効の確認
早老症モデルのklothoマウスとPAI-1ノックアウトマウスの交配により、血中P・Caに影響することなく、FGF23の血中濃度は抑制され、成長不全の解除や延命があることを見出している。そこで、複数の早老症モデルでの検証を行うため、klothoマウスとSAMマウスに対してPAI-1阻害薬TM5441ないしTM5484を経口投与し、

① PAI-1, Fgf23、Igfbp3, Ink4a, Sirt, Wrnといった老化関連遺伝子の発現を腎臓や血管での発現に対する効果を調べる。
② 血中PAI-1濃度及びFgf23濃度、カルシウム濃度、リン濃度に対する効果を調べる。
③ 体重増加及び生存期間に対する効果を調べる。
④ 腎機能や血圧に対する効果を調べる。
⑤ 腎臓や血管等組織における老化関連β ガラクトシダーゼ活性を組織染色により調べる。
⑥ 老化アミロイドーシス、学習・記憶障害、老年性骨粗鬆症、白内障などの老化関連病態に対する効果を調べる。

さらに、早老症モデルとして一般的に利用されているBubR1H/HマウスやWRN欠損マウスを用いることも検討する。いずれのモデルにおいても、老化関連遺伝子発現の亢進を抑制しうるか否かを指標としたスクリーニングをまず行う。指標となる遺伝子の発現に効果が認められた場合は、寿命をエンドポイントとして更に効果を確認するとともに、血液学的パラメータや組織レベルの老化に対する効果の有無を調べる。

メカニズムの解析と並行し、化合物の合成（大量合成法の検討を含む）とヒトでの安全性を予測する目的で非臨床一般毒性試験（サル単回及び２週間反復経口投与、non-GLP）を実施する。

（倫理面への配慮）

動物実験は動物福祉の立場からの要請や法的規制に充分従い、個体に最も負担の少ない実験手技を用いる。具体的には、東北大学の動物実験専門委員会に本課題にそった申請・承諾を得て、それぞれの「動物実験等に関する規程」に従って施行するので、動物倫理上も問題がない。また、遺伝子組換え実験については、「遺伝子組換え実験申請書」を提出し、承認を得た上で、法・規制に順じた措置を講じて研究を進める。

ICH（日米EU医薬品規制調和国際会議）で新薬承認審査の基準を国際的に統一し、医薬品の特性を検討するための非臨床試験・臨床試験の実施方法やルール等が取りまとめられている項目については、そのガイドラインやガイダンスを遵守して実施する。
GLP非臨床試験は、「医薬品の安全性に関する非臨床試験の実施の基準に関する省令」（厚生省令第21号：平成9年3月26日、一部改正　厚生労働省令第114号　平成20年6月13日）と「医薬品の安全性に関する非臨床試験の実施の基準に関する省令の一部を改正する省令による改正後の医薬品の安全性に関する非臨床試験の実施の基準に関する省令の取扱いについて」（薬食発第0613007号：平成20年6月13日付厚生労働省医薬食品局長通知）を遵守して実施する。その他、非臨床試験に関して法・規制基準があるものについても遵守する。

ヒトゲノム・遺伝子研究の実施にあたっては「ヒトゲノム・遺伝子解析研究に関する倫理指針」を、臨床研究の実施にあたっては「臨床研究に関する倫理指針」など関連する指針を遵守し、研究対象者に対する人権擁護を基本とし、インフォームドコンセントに基づいた科学的にも倫理的にも妥当な研究の計画と実施を心がける。

Ｃ．研究結果

本研究では、経口PAI-1阻害薬の実用化を目指した非臨床GLP試験までに必要な基礎研究をklotho欠損マウスにおける研究を中心に2年間で行う計画であった。しかし、下記に示すように、平成26年度にほぼ当初の計画を達成する成果を上げた。

① klotho欠損マウスにおいてPAI-1阻害により、IGFBP3の血中濃度は低下し、肝臓、腎臓等のTRLの発現低下は寛解した。PAI-1の遺伝子発現は腎臓、肺に加え大動脈においてklotho欠損により顕著に増加したが、PAI-1の阻害により寛解した。腎臓における老化マーカー遺伝子p16link4aの発現レベルも有意に低下した。また、抗Nω -nitro-L-arginine methyl ester（L-NAME：NO合成酵素の阻害によって老化を促進すると見られる）投与によるラット血管老化惹起モデルに対して、PAI-1阻害薬TM5441投与により、血管のp16link4aの発現上昇が顕著に抑制された。また、肝臓や大動脈におけるATLRの発現低下が有意に抑制された。
② Klotho欠損による血中FGF23上昇(295,657 pg/dL)は、PAI-1阻害により有意な抑制(3,795 pg/dL)が認められた。血中カルシウムおよびリン濃度については、PAI-1阻害による影響は認められなかった。

③ TM5441の経口投与により、klotho欠損に起因する体重減少は回復し、生存期間についても有意に延長し、最大でklotho欠損マウスの倍以上の300日程度まで生存した（論文発表２、Appendix1）。腎機能の指標である血中クレアチニンは、klotho欠損により高値となるが(0.31 mg/dL)、PAI-1阻害により、野生型同様の値まで低下した(0.18 mg/dL)。更に、上述のL-NAME投与モデルの血管老化に伴う高血圧は、TM5441経口投与による有意な軽減が認められた。

④ TM5441は、変異原性試験（Ames試験）では陰性であったが、染色体異常試験は陽性となった。TM5441のサル4週間毒性試験における無影響量（NOAEL）が10 mg/kg/dayであったのに対して、TM5484のサル２週間毒性試験のNOAELは10 mg/kg/day以下であった。なお、今後の対象組織である骨や肺への移行性が高いTM5509の誘導体のTM5614のラベル体を合成して、計画を約半年前倒しとして、^{14}C標識化合物の合成と薬物代謝や組織への移行性の検討を進めている。

D．考察

上記の一連の解析から、老化に伴う様々なバイオマーカーに対するPAI-1阻害薬の多面的な治療寛解効果を確認することが出来た。これに基づき、今後はウェルナー症候群をはじめとする早老症のみならず、骨粗しょう症や肺気腫・肺線維症といった老化に関連する疾患に対するPAI-1阻害薬の治療効果や作用機序の解析を行う予定である。

E．結論

当初計画のklotho欠損マウスを中心にした2年間の研究計画は、平成26年度でほぼ達成した。今後はウェルナー症候群をはじめとする早老症のみならず、骨粗しょう症や肺気腫・肺線維症といった老化に関連する疾患に対するPAI-1阻害薬の治療効果や作用機序の解析を行う予定である。

F．健康危険情報

健康危険情報はない。

G．研究発表

1．論文発表

1. Ibrahim AA, Yahata T, Onizuka M, Dan T, van Ypersele de Strihou C, Miyata T, Ando K. Inhibition of Plasminogen Activator Inhibitor Type-1 Activity Enhances Rapid and Sustainable Hematopoietic Regeneration. Stem Cells. 2014; 32: 946-58
2. Eren M, Boe A, Murphy SB, Place AT, Nagpal V, Morales-Nebreda L, Urich D, Quaggin SE, Budinger GS, Mutlu GM, Miyata T, Vaughan DE. PAI-1-regulated extracellular proteolysis governs senescence and survival in Klotho mice. Proc Natl Acad Sci USA. 2014; 111: 7090-7095.
3. Kimura H, Tanaka K, Kanno M, Watanabe K, Hayashi Y, Asahi K, Suzuki H, Sato K, Sakaue M, Terawaki H, Nakayama M, Miyata T, Watanabe T. Skin Autofluorescence Predicts Cardiovascular Mortality in Patients on Chronic Hemodialysis. Therapeutic Apheresis and Dialysis. 2014;18:461-7.
4. Jo-Watanabe A, Ohse T, Nishimatsu H, Takahashi M, Ikeda Y, Wada T, Shirakawa JI, Nagai R, Miyata T, Nagano T, Hirata Y, Inagi R, Nangaku M. Glyoxalase I reduces glycative and oxidative stress and prevents age-related endothelial dysfunction through modulation of endothelial nitric oxide synthase phosphorylation. Aging Cell. 2014; 13: 519-28.
5. Miyashita M, Arai M, Kobori A, Ichikawa T, Toriumi K, Niizato K, Oshima K, Okazaki Y, Yoshikawa T, Amano N, Miyata T, Itokawa M. Clinical features of schizophrenia with enhanced carbonyl stress. Schizophr Bull. 2014; 40: 1040-6.
6. Jung I, Piao L, Huh JY, Miyata T, Nam D, Ha H. A novel PAI-1 inhibitor, TM5441, protects high fat diet-induced obesity and adipocyte injury in mice. In press.
7. Kobayashi N, Ueno T, Ohashi K, Yamashita H, Takahashi Y, Sakamoto K, Manabe S, Hara S, Takashima Y, Dan T, Pastan I, Miyata T, Kurihara H, Matsusaka T, Reiser J, Nagata M. Podocyte injury-driven intracapillary plasminogen activator inhibitor type 1 accelerates podocyte loss via beta 1 integrin endocytosis. Am J Physiol Renal Physiol. Epub ahead of print.
8. Placencio VR, Ichimura A, Miyata T, DeClerck YA. Small Molecule Inhibitors of PAI-1 TM5275 and TM5441 Elicit Anti-Angiogenic and Anti-tumorigenic. Journal Molecular Cancer Therapeutics. In press.
9. Miyashita M, Watanabe T, Arai M, Ichikawa T, Toriumi K, Kobori A, Kushima I, Hashimoto R, Fukumoto M, Koike S, Ujike H, Arinami T, Tatebayashi Y, Kasai K, Takeda M, Ozaki M, Okazaki Y, Yoshikawa T, Ama

no N, Yamamoto H, Miyata T, Itokawa M. Identification of functional variants in AGER associated with a marked decrease in serum esRAGE levels. Journal of Human Genetics. In press.
10. Boe AE, Eren M, Morales-Nebreda L, Murphy SB, Budinger GR, Mutlu GM, Miyata T, Vaughan DE. Nitric oxide prevents alveolar senescence and emphysema in a mouse model. PLoS One. 2015; 10: e0116504.

2. 学会発表

1. Miyata T. Drug discovery in kidney disease: From serendipity to rationality. ISN Nexus Symposium: New era of drug discovery and clinical trials in kidney disease in Bergamo (Italy). 2014 April 3-6.
2. 宮田敏男.　アカデミアからの新薬開発：課題と展望.　革新ナノバイオデバイス研究センター特別セミナー（名古屋大学大学院工学研究科）.　2014.5.9. 名古屋
3. 宮田敏男.　アカデミアからの新薬開発：課題と展望.　研究カンファレンス講演（京都大学医学部附属病院呼吸器内科学）.　2014.6.9.京都
4. Miyata T. Drug discovery : Role and significance of academia. The 13th Kitasato University-Harvard School of Public Health Symposium in Tokyo(Japan). 2014 July 4-5.
5. Miyata T. Drug discovery in kidney disease - From serendipity to rationality -. Karolinska-Tohoku Joint Symposium on Medical Sciences in Sendai(Japan). 2014 November 8-9.
6. 宮田敏男.　ドラッグディスカバリー ―アカデミアの役割と重要性―.　第11回DIA日本総会（東京ビックサイト）.　2014.11.17.東京
7. Miyata T. Drug discovery and development: Respective role of academia. Third International Conference on Innovative Biology, Medicine, and Engineering (ICIBME 2015) in Nagoya(Japan). 2015 January 15-16.

H. 知的財産権の出願・登録状況
（予定を含む。）

1. 特許取得　　なし
2. 実用新案登録　　なし
3. その他　　なし

PAI-1–regulated extracellular proteolysis governs senescence and survival in *Klotho* mice

Mesut Eren[a], Amanda E. Boe[a,b], Sheila B. Murphy[a,b], Aaron T. Place[a,b], Varun Nagpal[a,b], Luisa Morales-Nebreda[a], Daniela Urich[a], Susan E. Quaggin[a,b], G. R. Scott Budinger[a], Gökhan M. Mutlu[a], Toshio Miyata[c], and Douglas E. Vaughan[a,b,1]

[a]Department of Medicine and [b]Feinberg Cardiovascular Research Institute, Northwestern University Feinberg School of Medicine, Chicago, IL 60611; and [c]United Centers for Advanced Research and Translational Medicine, Tohoku University Graduate School of Medicine, Miyagi 980-8575, Japan

Edited* by David Ginsburg, University of Michigan Medical School, Ann Arbor, MI, and approved April 2, 2014 (received for review November 25, 2013)

Cellular senescence restricts the proliferative capacity of cells and is accompanied by the production of several proteins, collectively termed the "senescence-messaging secretome" (SMS). As senescent cells accumulate in tissue, local effects of the SMS have been hypothesized to disrupt tissue regenerative capacity. *Klotho* functions as an aging-suppressor gene, and *Klotho*-deficient (*kl/kl*) mice exhibit an accelerated aging-like phenotype that includes a truncated lifespan, arteriosclerosis, and emphysema. Because plasminogen activator inhibitor-1 (PAI-1), a serine protease inhibitor (SERPIN), is elevated in *kl/kl* mice and is a critical determinant of replicative senescence in vitro, we hypothesized that a reduction in extracellular proteolytic activity contributes to the accelerated aging-like phenotype of *kl/kl* mice. Here we show that PAI-1 deficiency retards the development of senescence and protects organ structure and function while prolonging the lifespan of *kl/kl* mice. These findings indicate that a SERPIN-regulated cell-nonautonomous proteolytic cascade is a critical determinant of senescence in vivo.

FGF23 | IGFBP3 | IL-6 | TM5441

Advanced age contributes to the development of frailty and disease in humans, but the fundamental mechanisms that drive physiological aging are incompletely understood (1, 2). Cellular senescence, which halts the proliferative capacity of cells, is associated with the manifestation of the senescence-associated secretory phenotype (3) and the production and secretion of a distinct set of proteins (2, 4), including insulin-like growth factor-binding proteins (IGFBPs), interleukins (ILs), transforming growth factor type β (TGF-β), and plasminogen activator inhibitor-1 (PAI-1) (5), collectively termed the "senescence-messaging secretome" (SMS) (6). In addition to this pattern of protein production and secretion, senescent cells display a distinctive morphology, and can be identified by increased expression of senescence-associated β-galactosidase (7). The tumor suppressor and proapoptotic protein p53 plays a central role in inducing replicative senescence by regulating the transcription of genes involved in cell cycle arrest and apoptosis, including the cyclin-dependent kinase inhibitors $p16^{Ink4a}$ and p21 (8). Senescence can be triggered by a number of factors, including DNA damage (9), oncogene induction (10), and oxidative stress (11). Although the relationship between cellular senescence and physiological aging remains an area of intense investigation, it is becoming increasingly evident that the two processes are fundamentally linked. Senescent cells accumulate in aging tissues and have been hypothesized to disrupt tissue regeneration, which may reflect cell-nonautonomous effects of the SMS (6).

In the last decade, numerous examples of genetically modified mice with phenotypes reminiscent of human aging have been described and investigated. These include the $BubR1^{H/H}$ progeroid (12) and *Klotho*-deficient (*kl/kl*) mice (13). $BubR1^{H/H}$ progeroid mice exhibit an age-dependent increase in the expression levels of PAI-1 in numerous locations, including white adipose tissue, skeletal muscle, and the eye (12). $BubR1^{H/H}$ mice have a shortened average lifespan (24 wk) and develop various aging-like phenotypic abnormalities, including sarcopenia, cataracts, arterial stiffening, and impaired wound healing (14). Klotho functions as an aging-suppressor protein by impeding the development of senescence in vitro and in vivo through inhibition of the Wnt (15), TGF-β (16), and IGF1 signaling pathways (17). Thus, *kl/kl* mice exhibit a rapidly progressive phenotype after weaning that includes a truncated lifespan (8–12 wk), renal sclerosis, arteriosclerosis, emphysema, and osteoporosis (13). Membrane-bound Klotho forms a heterodimer with fibroblast growth factor (FGF) receptors (FGFRs) generating a high-affinity receptor for FGF23. Signals transduced by FGF23 via the Klotho–FGFR complex inhibit 1,25-$(OH)_2$ vitamin D_3 and parathyroid hormone synthesis and promote renal phosphate excretion. *kl/kl* mice exhibit a remarkable increase in plasma levels of FGF23, as well as significant increases in serum levels of calcium, phosphate, vitamin D_3, and creatinine (13). Interestingly, *kl/kl* mice also have an age-dependent increase in plasma PAI-1 levels as well as increased PAI-1 expression in a number of tissues including kidney, aorta, and heart (18). Because PAI-1 is necessary and sufficient to induce replicative senescence in vitro downstream of p53 (19) and is markedly increased in *kl/kl* mice, we hypothesized that PAI-1 is a critical determinant of the phenotypic abnormalities developed by *kl/kl* mice. Here we examined the impact of PAI-1 on senescence and physiological aging in vivo by breeding *kl/kl* and PAI-1–deficient ($pai\text{-}1^{-/-}$) mice to generate *kl/kl* mice with partial ($kl/klpai\text{-}1^{+/-}$) or complete ($kl/klpai\text{-}1^{-/-}$) PAI-1 deficiency.

Results

PAI-1 Deficiency Prolongs the Survival of *kl/kl* Mice. We systematically monitored the effect of PAI-1 deficiency on the growth, vigor, and survival of littermate *kl/kl* ($n = 26$), $kl/klpai\text{-}1^{+/-}$ ($n = 39$), $kl/klpai\text{-}1^{-/-}$ ($n = 25$), and WT ($n = 16$) mice (Fig. 1) all in the

Significance

Plasminogen activator inhibitor-1 (PAI-1) is an essential mediator of cellular senescence in vitro and is one of the biochemical fingerprints of senescence in vivo. *Klotho*-deficient (*kl/kl*) mice display a complex phenotype reminiscent of human aging and exhibit age-dependent increases in PAI-1 in tissues and in plasma. Thus, we hypothesized that PAI-1 contributes to the aging-like phenotype of *kl/kl* mice. We observed that either genetic deficiency or pharmacological inhibition of PAI-1 in *kl/kl* mice was associated with reduced evidence of senescence, preserved organ structure and function, and a fourfold increase in median lifespan. These findings indicate that PAI-1 is a critical mediator of senescence in vivo and defines a novel target for the prevention and treatment of age-related disorders in man.

Author contributions: M.E. and D.E.V. designed research; M.E., A.E.B., S.B.M., A.T.P., V.N., L.M.-N., and D.U. performed research; T.M. contributed new reagents/analytic tools; M.E., S.E.Q., G.R.S.B., G.M.M., and D.E.V. analyzed data; and M.E. and D.E.V. wrote the paper.

The authors declare no conflict of interest.

*This Direct Submission article had a prearranged editor.

[1]To whom correspondence should be addressed. E-mail: d-vaughan@northwestern.edu.

This article contains supporting information online at www.pnas.org/lookup/suppl/doi:10.1073/pnas.1321942111/-/DCSupplemental.

same genetic background (75% C57BL/6J, 25% C3J). We observed that either partial or complete absence of PAI-1 prolonged the survival of *kl/kl* mice. Log-rank analysis indicated that the survival curves for the WT, *kl/kl*, *kl/klpai-1*$^{+/-}$, and *kl/klpai-1*$^{-/-}$ mice differed significantly ($P < 0.0001$). The median survival of *kl/kl* mice was 58 d, and this value increased with PAI-1 deficiency: 2.8-fold (163 d) in *kl/klpai-1*$^{+/-}$ mice and 4.2-fold (246 d) in *kl/klpai-1*$^{-/-}$ mice. Whereas all of the *kl/kl* mice died within 120 d, 65% of *kl/klpai-1*$^{+/-}$ and 82% of *kl/klpai-1*$^{-/-}$ mice were alive beyond 120 d. Although median survival indicates a dose–response relationship between genotype and mortality ($P = 0.0002$ by log-rank test for trend), the mean lifespan increased similarly in *kl/klpai-1*$^{+/-}$ (250 ± 169 d) and *kl/klpai-1*$^{-/-}$ (254 ± 123 d) mice (mean ± SD), corresponding to 4.2- and 4.5-fold increases, respectively. Furthermore, we achieved a similar prolongation of lifespan in *kl/kl* mice ($n = 11$) (Fig. 1*B*) by the administration of an orally active small-molecule PAI-1 antagonist, TM5441, whose pharmacokinetic properties, toxicity, and specificity have been described recently (20). In contrast with the inconsistent effects based on sex of a low phosphate diet on survival in *kl/kl* mice (21), both males and females appear to benefit from complete PAI-1 deficiency. However, survival of *kl/klpai-1*$^{+/-}$ females ($n = 19$) was not as long as that of males ($n = 20$) of the same genotype (median survival 121 d vs. 315 d, mean lifespan 208 ± 151 d vs. 285 ± 182, respectively; $P = 0.16$). Nevertheless, *kl/klpai-1*$^{+/-}$ females do live longer than *kl/kl* females ($n = 14$) (median survival 121 d vs. 58 d, mean lifespan 208 ± 151 d vs. 57 ± 18, respectively; $P = 0.0004$) (Fig. S1). This improvement in survival was also associated with evidence of increased overall vigor and health, as *kl/klpai-1*$^{-/-}$ mice exhibited near-normal weight gain over time (Fig. 1 *A* and *C*) and spontaneous physical activity (Fig. 1*D*).

PAI-1 Deficiency Normalizes Senescence and Telomere Length in *kl/kl* Mice. To characterize the extent of senescence in *kl/kl* mice and how PAI-1 deficiency affects it, plasma levels of the SMS factors IGFBP-3 and IL-6, and telomere length were measured in liver, aorta, tail, and kidney tissue. We observed that *kl/kl* mice had increased levels of IGFBP-3 (Fig. 2*A*) compared with WT mice ($P = 0.02$). With partial ($P = 0.03$ vs. *kl/kl* mice) or complete PAI-1 deficiency ($P = 0.02$ vs. *kl/kl* mice), IGFBP-3 levels did not significantly differ from those seen in WT mice. Similarly, we found that compared with levels in WT mice, *kl/kl* mice had a 13-fold increase ($P = 0.02$) in plasma levels of proinflammatory cytokine IL-6, which functions in the acquisition of the senescent phenotype in vitro (Fig. 2*B*). Compared with *kl/kl* mice, IL-6 levels were reduced by 79% in *kl/klpai-1*$^{+/-}$ ($P = 0.03$) and 83% in *kl/klpai-1*$^{-/-}$ ($P = 0.0001$) mice. These observations suggest that the elevated PAI-1 levels in *kl/kl* mice are a dominant factor in contributing to increases in plasma IGFBP-3 and IL-6 and further augment the senescent phenotype in these mice.

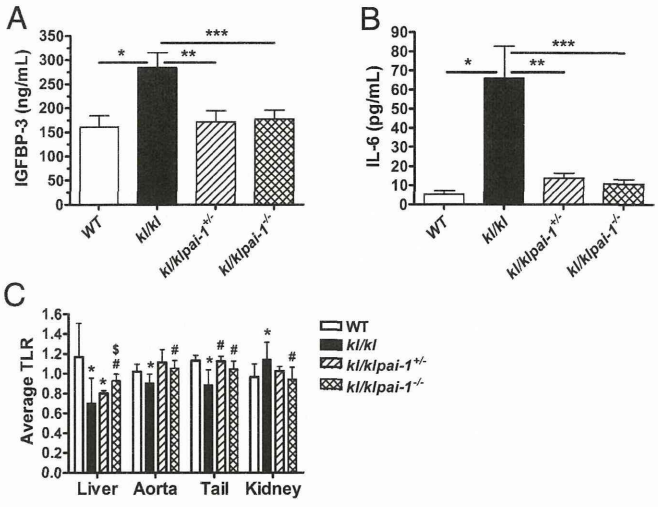

Fig. 2. Effect of PAI-1 deficiency on plasma levels of SMS factors and ATLR in various tissues from age-matched littermate *Klotho* mice. (*A*) Determination of IGFBP-3 levels in plasma samples ($n = 6$ per group). *$P = 0.02$, **$P = 0.03$, and ***$P = 0.02$. (*B*) Quantitation of circulating IL-6 levels ($n = 6$ to 14). *$P = 0.02$, **$P = 0.03$, and ***$P = 0.0001$. (*C*) Quantitation of ATLR by qRT-PCR in liver, aorta, tail, and kidney tissue ($n = 6$ to 14). *$P < 0.05$ compared with WT, #$P < 0.05$ compared with *kl/kl*, and $P < 0.05$ compared with *kl/klpai-1*$^{+/-}$. Data are plotted as mean ± SD.

Although elevated plasma levels of SMS components may reflect systemic senescence, they are nonspecific in nature and do not provide precise identification of which tissues are actually senescent. To address this limitation, telomere length was determined in several different tissues. Liver, aorta, and tail tissue samples from *kl/kl* mice displayed moderate but significant decreases in the average telomere length ratio (ATLR), whereas renal tissue had 16% longer ATLRs compared with those of WT animals (Fig. 2*C*). In contrast, ATLRs of liver and tail tissues from *kl/klpai-1*$^{+/-}$ and liver, aorta, and tail, tissues from *kl/klpai-1*$^{-/-}$ mice were significantly longer than those of *kl/kl* mice. These findings indicate that PAI-1 deficiency provides partial protection of telomere integrity in numerous tissues. The anomalous

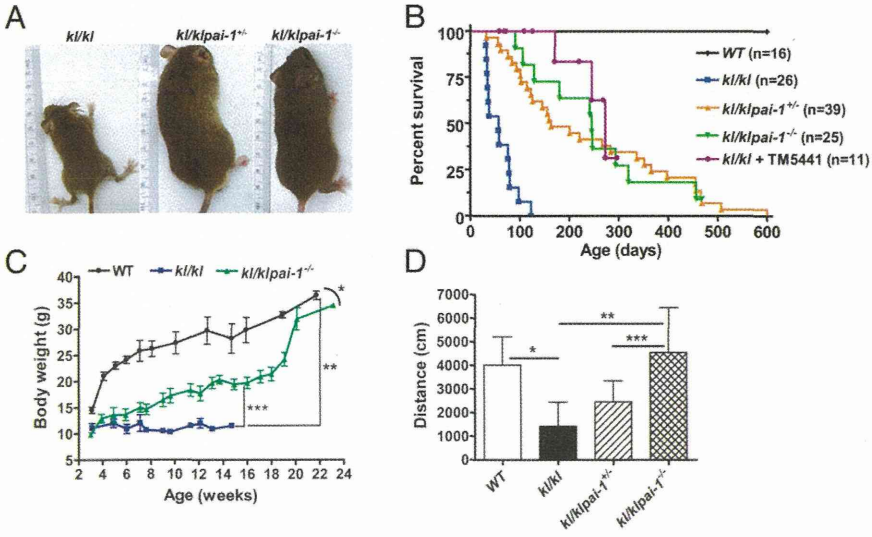

Fig. 1. Effects of PAI-1 deficiency in *Klotho* mice. (*A*) Size and appearance of 8-wk-old littermate mice. (*B*) Survival curve. Log-rank analysis showed that the survival curves for the WT, *kl/kl*, *kl/klpai-1*$^{+/-}$, and *kl/klpai-1*$^{-/-}$ mice differed significantly ($P < 0.0001$). (*C*) Bodyweight measurements starting from 3 wk of age. *$P = 0.002$, **$P = 0.0001$, and ***$P = 0.0003$. (*D*) Open field physical activity measurements recorded as distance traveled in 20 min in age-matched animals. *$P = 0.027$, **$P = 0.018$, and ***$P = 0.036$. Data are plotted as mean ± SD.

preservation of telomere length in renal tissue from *kl/kl* mice may reflect the lack of turnover in renal cells and the early induction of replicative senescence in the kidneys of *kl/kl* mice (22).

Because the kidneys are one of the most severely compromised organs in *kl/kl* mice, we also examined kidneys for biomarkers of senescence, including $p16^{Ink4a}$ and p21. We detected strong immunostaining for $p16^{Ink4a}$ localized in the nuclei of tubules in kidney tissues from *kl/kl* mice (Fig. 3), but not for p21. In contrast, kidney sections from *kl/klpai-1*$^{-/-}$ mice had only minimal evidence of $p16^{Ink4a}$ accumulation (Fig. 3). Quantitative real-time PCR (qRT-PCR) analysis showed that the relative expression of $p16^{Ink4a}$ in kidneys from *kl/kl* mice is 3.2-fold higher than that in WT mice ($P = 0.001$) (Fig. 3*E*). In *kl/klpai-1*$^{+/-}$ and *kl/klpai-1*$^{-/-}$ mice, $p16^{Ink4a}$ expression was reduced by 80% ($P = 0.04$) and 92% ($P = 0.0001$) compared with the *kl/kl* mice, respectively, and in *kl/klpai-1*$^{-/-}$ mice by 78% compared with the levels seen in WT animals ($P = 0.0001$).

Effect of PAI-1 Deficiency on the Biochemical Hallmarks of *kl/kl* Mice. In an effort to explain the effects of PAI-1 deficiency on the *kl/kl* phenotype, we measured plasma levels of factors that are biochemical hallmarks of *kl/kl* mice, including FGF23, vitamin D_3, calcium, phosphate, creatinine, and PAI-1 (Table 1). As expected, *kl/kl* mice displayed a more than 1,200-fold increase in FGF23 levels [$2.8 \times 10^5 \pm 1.4 \times 10^5$ pg/mL vs. 225 ± 65 pg/mL in WT mice ($P = 0.004$)], reflecting the loss of functioning receptors for FGF23. Both *kl/klpai-1*$^{+/-}$ and *kl/klpai-1*$^{-/-}$ mice exhibited a nearly 98% reduction in plasma FGF23 levels compared with *kl/kl* mice [$3.4 \times 10^3 \pm 2.1 \times 10^3$ pg/mL ($P < 0.0001$) and $3.9 \times 10^3 \pm 0.9 \times 10^3$ pg/mL ($P = 0.0001$), respectively]. Similarly, vitamin D_3 levels were reduced in *kl/klpai-1*$^{+/-}$ ($P = 0.032$) and *kl/klpai-1*$^{-/-}$ ($P = 0.0003$) mice compared with the levels in *kl/kl* mice. Interestingly, partial or complete PAI-1 deficiency had only a marginal impact on serum levels of calcium, phosphate, and creatinine in *kl/kl* mice. As expected, PAI-1 antigen was not detectable in plasma from *kl/klpai-1*$^{-/-}$ mice, and levels in *kl/klpai-1*$^{+/-}$ animals were reduced by nearly 50% compared with those from *kl/kl* mice ($P < 0.05$). In addition, PAI-1 expression levels were reduced in tissues from *kl/klpai-1*$^{+/-}$ mice compared with those of *kl/kl* mice (Fig. S2).

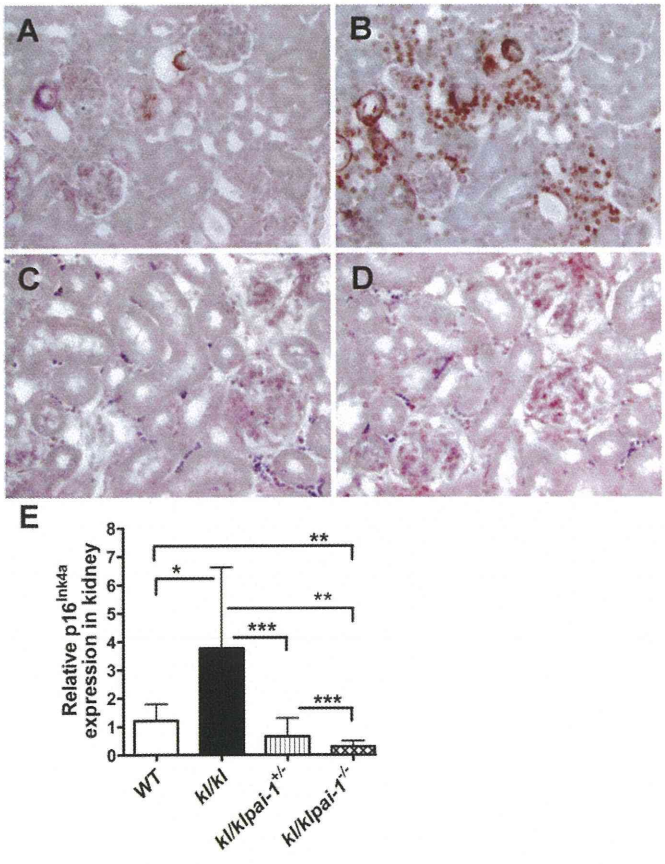

Fig. 3. Effect of PAI-1 deficiency on renal $p16^{Ink4a}$ expression in *Klotho*-deficient mice. (*A* and *C*) Control immunostaining of kidney sections from *kl/kl* and *kl/klpai-1*$^{-/-}$ mice, respectively, in the absence of the anti-$p16^{Ink4a}$ antibody. (*B* and *D*) Immunodetection of $p16^{Ink4a}$-positive cells in kidney sections from *kl/kl* and *kl/klpai-1*$^{-/-}$ mice, respectively. (*E*) Quantitation of relative $p16^{Ink4a}$ expression in the kidney. qRT-PCR analysis was performed on total RNA samples purified from WT ($n = 8$), *kl/kl* ($n = 6$), *kl/klpai-1*$^{+/-}$ ($n = 4$), and *kl/klpai-1*$^{-/-}$ ($n = 8$) kidneys. *$P = 0.001$, **$P = 0.0001$, and ***$P = 0.04$. Data are plotted as mean ± SD. (Magnification: *A–D*, 60×.)

PAI-1 Deficiency Preserves Organ Structure in *kl/kl* Mice. As reported previously, *kl/kl* mice develop emphysema that is characterized by a progressive, age-dependent enlargement of air spaces and associated alveolar destruction (Fig. 4) (23). Histological analysis of lung tissues from *kl/klpai-1*$^{+/-}$ and *kl/klpai-1*$^{-/-}$ (Fig. 4) mice showed that PAI-1 deficiency primarily prevents alveolar enlargement. Consistent with the preservation of pulmonary structural integrity, pulmonary function was also maintained with PAI-1 deficiency. We found that *kl/kl* mice had a 40% decrease in PaO_2 levels ($P = 0.018$) in arterial blood samples. Arterial oxygenation normalized with partial ($P = 0.05$) and complete ($P = 0.02$) PAI-1 deficiency in *kl/kl* mice (Fig. 4*E*). These results indicate that PAI-1 is an important contributor to the emphysematous changes observed in *kl/kl* mice.

Finally, we analyzed mice for evidence of ectopic calcification, which has been reported to increase with age in *kl/kl* mice. Whereas the age-matched WT littermate mice had no detectable calcification, we observed prominent calcium deposits in the kidneys of *kl/kl* mice (Fig. 5 *A* and *B*) ($P = 0.002$). However, analysis of kidneys from *kl/klpai-1*$^{+/-}$ (Fig. 5*C*) and *kl/klpai-1*$^{-/-}$ (Fig. 5*D*) mice showed that ectopic calcification areas were significantly reduced by 41% ($P = 0.03$) and 96% ($P < 0.0001$), respectively. To test the effect of PAI-1 deficiency on the impaired osteogenic signaling observed in *kl/kl* mice (24, 25), we measured the serum levels of aldosterone and alkaline phosphatase (ALP) activity (Table 1). Although aldosterone levels were significantly higher in *kl/kl* mice than that of WT animals, it was not altered significantly in *kl/klpai-1*$^{-/-}$ mice. Furthermore, we did not observe any difference in ALP activity among the mice groups studied here. This observation indicates that partial or complete loss of PAI-1 expression protects against age-induced ectopic calcification in *kl/kl* mice without altering serum levels of phosphate, calcium, ALP and aldosterone.

Discussion

PAI-1 is expressed in senescent cells and tissues, and is recognized as a primary component of the SMS. Most mammalian models of aging investigated thus far exhibit evidence of increased PAI-1 expression (12, 14). Furthermore, genetic or therapeutic interventions that prolong survival or reduce senescence in tissues in vivo are coincidentally associated with reductions in PAI-1. To our knowledge, this in vivo study is the first to investigate systematically the role of PAI-1 not only in the development of senescence, but also in the aging-like pathology of a mammal. The results from this study suggest that the onset of physiological aging can be delayed by modulating PAI-1, which subsequently prevents the nuclear accumulation of senescence marker $p16^{Ink4a}$ and maintains the structural and functional integrity of vital organs. Furthermore, the ability of a small-molecule PAI-1 antagonist to augment survival to a similar extent in *kl/kl* mice indicates that the observed effects are likely cell-nonautonomous. The protective effects of partial or complete PAI-1 deficiency are in agreement with previous work from our laboratory indicating that transgenic overexpression of

Table 1. Effects of PAI-1 deficiency on blood levels of the biochemical hallmarks of *klotho* mice

Circulating factors assayed	WT $n = 4$ to 5	*kl/kl* $n = 6$ to 9	*kl/klpai-1*$^{+/-}$ $n = 5$ to 6	*kl/klpai-1*$^{-/-}$ $n = 6$ to 10
Phosphate, mg/dL	7.7 ± 1.6	14.0 ± 2.8*	10.8 ± 2.6*	12.6 ± 2.7*
Calcium, mg/dL	7.9 ± 0.6	10.4 ± 0.9*	10.1 ± 1.2*	10.6 ± 0.8*
Creatinine, mg/dL	0.22 ± 0.11	0.31 ± 0.33	0.21 ± 0.11	0.18 ± 0.06
PAI-1, ng/mL	1.8 ± 0.4	45.2 ± 4.8*	24.3 ± 2.7*	0.0
FGF23, pg/mL	225 ± 65	295,657 ± 139,709*	3,924 ± 1,316*,#	3,795 ± 870*,#
Vitamin D_3, pg/mL	ND	1359 ± 145	698 ± 419#	314 ± 244#
Aldosterone, pg/mL	102 ± 20	160 ± 55*	ND	223 ± 96*
ALP, U/mL	20 ± 7	21 ± 6	17 ± 7	19 ± 5

ND, not determined.
*$P < 0.05$ compared with WT.
#$P < 0.05$ compared with *kl/kl*.

PAI-1 is sufficient to induce several aging-like phenotypic abnormalities, including age-dependent spontaneous coronary thrombosis, systemic amyloid deposition, and hair loss (26).

The normalization of FGF23 and vitamin D_3 levels in partial or complete PAI-1 knockout models strongly indicates that PAI-1 directly influences FGF23 signaling in *kl/kl* mice. Recent observations demonstrate that FGF23 is highly sensitive to cleavage by the serine protease furin, which is rapidly inhibited by PAI-1 (27, 28). In addition to FGF23, *kl/kl* mice have augmented expression of other furin substrates, including IGF1, TGF-β, MMP2, and MMP9 (29, 30). PAI-1 is known to regulate the proteolytic activation and/or clearance of many of these proteins. The precise identity and function of other proteases that are inhibited by PAI-1 and that contribute to the *Klotho* phenotype merits further investigation.

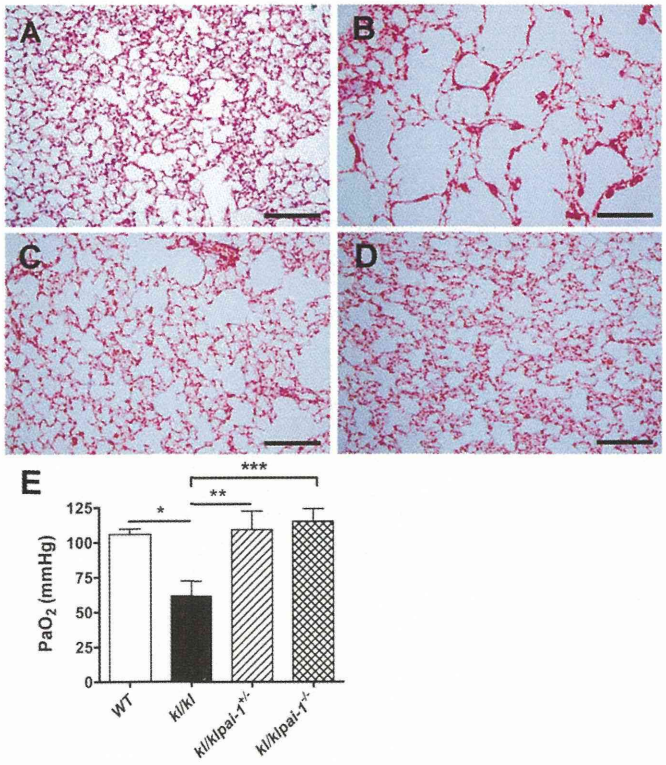

Fig. 4. Effects of PAI-1 deficiency on lung morphology and function. Masson's trichrome staining of lung sections in (*A*) WT, (*B*) *kl/kl*, (*C*) *kl/klpai-1*$^{+/-}$, and (*D*) *kl/klpai-1*$^{-/-}$ mice. (Scale bars: 150 μm.) (*E*) Partial pressure of oxygen (PaO_2) measurements in arterial blood ($n = 4$ for each group). *$P = 0.018$, **$P = 0.05$, and ***$P = 0.02$. Data are plotted as mean ± SD.

Because FGF23 signaling is impaired in *kl/kl* mice, the negative feedback inhibition on vitamin D_3 synthesis is dysfunctional. High vitamin D_3 and phosphate levels in *kl/kl* mice likely stimulate FGF23 synthesis in bone continuously, whereas the elevated PAI-1 levels reduce the proteolytic clearance of FGF23. Together, these combined effects on production, signaling, and metabolism likely explain the >1,200-fold increase in plasma FGF23 levels observed in *kl/kl* mice. Recent reports indicate that dietary deficiency of phosphate, zinc, and calcium significantly improves the lifespan of klotho mice (21, 25, 31). Although we did not detect any significant changes in the levels of phosphate and calcium in *kl/klpai-1*$^{-/-}$ mice, we observed that PAI-1 deficiency significantly prolongs the survival of *kl/kl* mice indicating that, in addition to the mineral homeostasis, PAI-1–regulated extracellular proteolysis strongly influences the aging phenotype.

Our findings also reveal a previously unrecognized role of PAI-1 in modulating the effects of FGF23. The increased plasma levels of PAI-1 in *kl/kl* mice are not surprising, but deserve some mechanistic explanation. Numerous factors likely contribute to the *Klotho* phenotype, and prominent on that list are the effects of TGF-β (16), Wnt (15), and IGF1 (17, 32). Importantly, all three of these factors can directly induce PAI-1 expression. As the phenotype matures, PAI-1 production is likely further augmented by the effects of progressive hypoxemia, the induction of the p53 pathway, aldosterone excess (25), and elevated levels of other components of the SMS, including IL-6, interferons, TGF-β, and IGFBPs.

Discovery of the *Klotho* gene has shed light into the molecular mechanisms of tissue calcification. The elevated phosphate and calcium levels in *kl/kl* mice certainly contribute to the pattern of ectopic calcification (33, 34). Recently, hyperaldosteronism was reported to be the major inducer of the osteog enic signaling, which was partially reversed by spironolactone without normalizing plasma levels of vitamin D_3, FGF23, calcium, and phosphate (24, 25). Furthermore, Lim et al. reported that FGF23 treatment reduced the aldosterone-induced expression of osteogenic factors in vitro (35). In addition, PAI-1 deficiency drastically reduced FGF23 levels and calcification without altering aldosterone and ALP levels in *kl/kl* mice (Table 1). These findings suggest that PAI-1, which is regulated by aldosterone (36), plays an unexpected but pivotal role in tissue calcification. The reduced plasma levels of vitamin D_3 and prevention of tissue calcification in *kl/klpai-1*$^{-/-}$ mice require the restoration of Klotho-independent FGF23 signaling. The present study strongly indicates that PAI-1 plays a direct role in the regulation of FGF23 signaling in *kl/kl* mice.

The reduced IGFBP-3 levels in *kl/kl* mice provide an important mechanistic insight into the protective effects of PAI-1 deficiency on the *Klotho* phenotype. It was recently demonstrated that the PAI-1–IGFBP-3 cascade promotes stress-induced senescence in human breast fibroblasts (37). Expression levels of IGFBP-3 are increased in response to senescence-inducing stimuli. However, the proteolytic metabolism of IGFBP-3 by tissue-type plasminogen activator (t-PA) prevents the induction of cellular

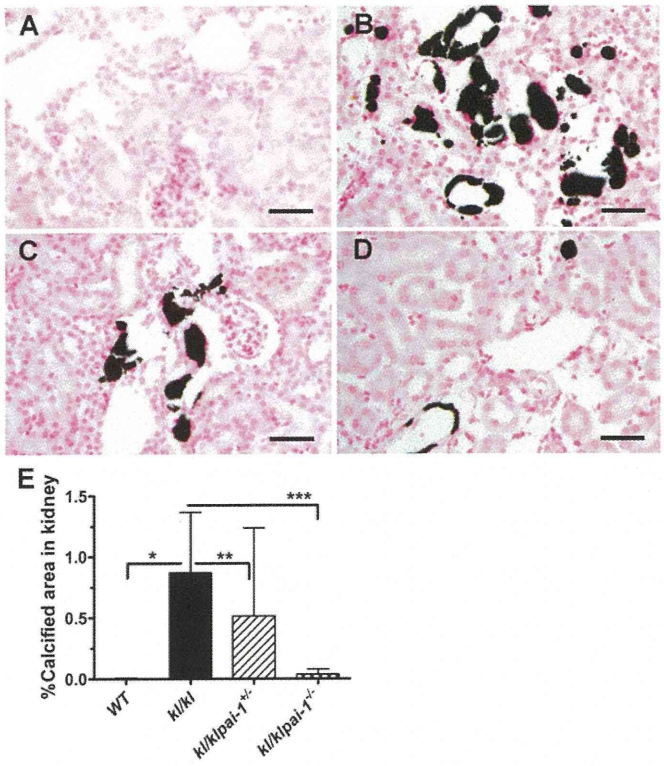

Fig. 5. Effects of PAI-1 deficiency on ectopic calcification characterized by von Kossa staining. Ectopic calcification analysis was performed on kidney ($n = 5$ for each group) sections. Although samples from (*A*) WT mice showed no detectable calcification, kidney sections from (*B*) *kl/kl* mice had remarkable calcified deposits. (*C*) Partial (*kl/klpai-1*$^{+/-}$) or (*D*) complete PAI-1 deficiency (*kl/klpai-1*$^{-/-}$), on the other hand, significantly decreased calcification levels. (Scale bars: 40 μm.) (*E*) Quantitative analyses using Image-Pro-6.3 software showed that the percentages of calcified areas in kidneys were reduced by 41% in *kl/klpai-1*$^{+/-}$ and 96% in *kl/klpai-1*$^{-/-}$ mice compared with *kl/kl* mice. $*P = 0.002$, $**P = 0.03$, and $***P = 0.0001$. Data are plotted as mean ± SD.

senescence in vitro. Because PAI-1 is the main physiological inhibitor of t-PA, IGFBP-3 appears to be a critical downstream target of PAI-1–induced senescence. These findings provide a possible mechanistic explanation for the prosenescent effects of increased PAI-1 in *kl/kl* mice and suggest a role for an extracellular cascade of secreted proteins in the regulation of cellular senescence and physiological aging.

It was recently shown that membrane-bound Klotho prevents the retinoic-acid-inducible gene-I–induced expression of IL-6 and -8 both in vitro and in vivo, suggesting that the antiaging function of Klotho also includes the suppression of inflammation (38). It is interesting to note that with PAI-1 deficiency, levels of both IGFBP-3 and IL-6 were normalized in *kl/kl* mice. This confirms and extends the recent observations by López-Andrés et al. that modulating the activity of a key member of the SMS can also normalize the levels of other SMS factors (39). This indicates that IGFBP-3 and IL-6 are downstream from PAI-1 in the senescence pathway.

In human fibroblasts, telomere shortening initiates senescence through a pathway that involves ataxia telangiectasia mutated (ATM), p53, and $p21^{CIP1}$, but not $p16^{Ink4a}$ (9). Thus, the presence of $p16^{Ink4a}$-positive but not p21-positive cells in kidneys of *kl/kl* mice suggests that the pathway to senescence and accelerated aging in the renal tissue of *kl/kl* mice is likely mediated by $p16^{Ink4a}$ and occurs independently of the p53 pathway. These findings in the kidney of preserved telomere length, together with augmented $p16^{Ink4a}$ expression, suggest that renal cells undergo senescence without the requisite cellular division to shorten telomeres (22).

The results presented here indicate that PAI-1 is a critical contributor to, and not merely a marker of, senescence in vivo (12), and that novel therapies targeting PAI-1 or other components of the SMS (40) may prevent senescence and age-related pathologic changes in humans, including arteriosclerosis and emphysema. The development of small-molecule, orally active, selective PAI-1 antagonists, such as TM5441 and others (41), will allow these hypotheses to be tested prospectively.

Materials and Methods

Animals and Animal Care. The original genetic background of *kl/kl* mice, a kind gift from Makoto Kuro-o (Jichi Medial University, Shimotsuke, Tochigi, Japan), was composed of C57BL/6J and C3H/J (13). PAI-1–deficient mice were obtained from The Jackson Laboratory (background strain C57BL/6J; strain name B6.129S2-Serpine1tm1Mlg/J; stock no. 002507). *Klotho* mice and PAI-1–deficient mice were crossed to generate the heterozygous dihybrid mice (*KL/kl-pai-1*$^{+/-}$). All mice used in this study were littermates generated by breeding these *KL/kl-pai-1*$^{+/-}$ mice and thus of the same mixed background. They were housed in a temperature-controlled environment with a daily 14:10 h light–dark cycle and had unlimited access to food (standard rodent chow diet; Harlan Teklad) and water. All experimental protocols were approved by the Institutional Animal Care and Use Committee of Northwestern University.

PAI-1 Inhibitor TM5441. TM5441 was derived from the original hit compound TM5007 (42) and the lead compound TM5275 (43) through an extensive structure-activity relationship (44). We have recently described the pharmacokinetic properties and toxicity, and specificity of TM5441 (20). TM5441 was administered at 100 mg/kg·d^{-1} mixed in the chow.

Histological Methods. Tissues harvested from mice were fixed in formalin for 24–48 h and then processed overnight and embedded in paraffin. Tissues sectioned at 6-μm thickness were stained with Masson's trichrome to visualize tissue morphology. Ectopic calcification was analyzed by von Kossa staining of kidneys ($n = 5$ for each study group). The extent of calcification was quantified in multiple kidney sections from each mouse by using Image-Pro-6.3 image-processing software and the results presented as the percent calcified areas in kidneys (Fig. 3). To detect the senescent cells, tissue sections were immunostained overnight at 4 °C with a primary antibody to $p16^{Ink4a}$ antigen (Cell Applications), and then the antigen was visualized with an HRP-conjugated secondary antibody (goat anti-mouse IgG at 1:500 dilution; Santa Cruz Biotechnology, Inc.). One-Step AEC Solution (BioGenex) was used as the substrate for antigen detection.

Quantitation of Factors in Plasma and Serum. Plasma levels of IGFBP-3, IL-6, and FGF23 were measured using the ELISA kits Quantikine Immunoassay kit from R&D Systems (catalog no. MGB300), Becton-Dickinson (catalog no. 555220), and Immutopics (catalog no. 60-6300), respectively, by following the manufacturers' suggested protocols. Vitamin D_3 levels in plasma were measured using the mouse 1,25-$(OH)_2$VitD3 HVD3 ELISA kit from NovaTein Biosciences (catalog no. NB-E20523). Calcium (catalog no. 0150-250), creatinine (catalog no. 0430-120), and phosphate (catalog no. 0830-125) levels were determined by using kits from Stanbio Laboratories. Plasma PAI-1 levels were measured with the Murine PAI-1 Total Antigen Assay from Molecular Innovations. A colorimetric assay kit and an ELISA kit from Abcam were used to measure serum levels of ALP and aldosterone (catalog nos. ab83369 and ab136933, respectively).

Measuring Partial Oxygen Pressure in Arterial Blood. PaO_2 levels in the arterial blood were measured in mice anesthetized with pentobarbital (75 mg/kg body weight, administered i.p.). After adequate anesthesia was achieved, we performed a tracheostomy and sutured a 20-gauge angiocatheter into the trachea. Mice were then placed on a small rodent ventilator (MiniVent; Harvard Apparatus) with the following settings: a respiratory rate of 150 breaths per minute, a tidal volume of 8 mL/kg body weight, and an FiO_2 of 0.21 (room air) as described previously (45). The animals were ventilated for 15 min before a thoracotomy was performed and then 200 μL arterial blood were collected into a heparinized syringe via direct puncture of the left ventricle. The arterial blood sample was processed for gas analysis using the Stat Profile pHOx blood gas analyzer (Nova Biomedical).

Quantitation of ATLR. Genomic DNA isolated from various tissues was used to measure telomere length by qRT-PCR as previously described with minor modification (46, 47). Briefly, telomere repeats were amplified using specially designed primers, which were then compared with the amplification of

a single-copy gene, the 36B4 gene (acidic ribosomal phosphoprotein PO), to determine the ATLR. One hundred nanograms of genomic DNA template were added to each 20 μL reaction containing forward and reverse primers (250 nM each for telomere primers, and 500 nM each for the 36B4 primers), SsoAdvanced SYBR Green Supermix (Bio-Rad USA), and nuclease-free water. A serially diluted standard curve of 100 ng to 3.125 ng per well of template DNA from a WT mouse sample was included on each plate for both the telomere and the 36B4 reactions to facilitate ATLR calculation. Critical values were converted to nanogram values according to the standard curves, and nanogram values of the telomere (T) reaction were divided by the nanogram values of the 36B4 (S) reaction to yield the ATLR. The primer sequences for the telomere portion were as follows: 5′-CGG TTT GTT TGG GTT TGG GTT TGG GTT TGG GTT-3′ and 5′-GGC TTG CCT TAC CCT TAC CCT TAC CCT TAC CCT TAC CCT-3′. The primer sequences for the 36B4 single copy gene portion were as follows: 5′-ACT GGT CTA GGA CCC GAG AAG-3′ and 5′-TCA ATG GTG CCT CTG GAG ATT-3′. Cycling conditions for both primer sets (run in the same plate) were 95 °C for 10 min, 30 cycles of 95 °C for 15 s, and 55 °C for 1 min for annealing and extension.

qRT-PCR. Tissues harvested from subject mice were snap-frozen in liquid nitrogen. Excess tissue was removed under a dissecting microscope. RNA was isolated using the Qiagen RNAeasy Mini Kit (Qiagen) using the manufacturer's protocol. cDNA was generated from the RNA using the qScript cDNA Supermix (Quanta Biosciences). qRT-PCR was performed using the SsoAdvanced SYBR Green Supermix (Bio-Rad USA). Forward and reverse primers used for $p16^{Ink4a}$ expression were, respectively: 5′-AGGGCCGTGTGCATGACGTG-3′ and 5′-GCACCGGGCGGGAGAAGGTA-3′; for PAI-1 expression, respectively: 5′-ACGCCTGGTGCTGGTGAATGC-3′ and 5′-ACGGTGCTGCCATCAGACTTGTG-3′; and for GAPDH expression, respectively: 5′-ATGTTCCAGTATGACTCCACTCACG-3′ and 5′-GAAGACACCAGTAGACTCCACGACA-3′ (IDT, Inc.).

Behavioral Characterization. To test the effect of PAI-1 deficiency on the level of physical activity of *kl/kl* mice, the open field test for spontaneous horizontal activity was performed on age-matched animals at the Northwestern University Mouse Behavioral Phenotyping Core Laboratory as described previously (13).

Statistical Analyses. We present the averaged values obtained for each study as mean ± SD. Statistical significance was assigned to a comparison by using an unpaired, two-tailed Student *t* test when comparing two groups. Statistical significance for the survival of groups was established by the log-rank analysis of Kaplan–Meier plots using GraphPad Prism 4 software. $P < 0.05$ was considered statistically significant.

ACKNOWLEDGMENTS. We thank Dr. Makoto Kuro-o for providing us with the *kl/kl* mice. We also thank Marissa Michaels for her help in obtaining reagents and coordinating various aspects of our projects. This work was supported by National Institutes of Health (NIH)/National Heart, Lung, and Blood Institute Grants 2R01HL051387 and 1P01HL108795. A.T.P. is supported in part by NIH National Institute of Diabetes and Digestive and Kidney Diseases Training Grant T32 KD007169.

1. Rodier F, Campisi J (2011) Four faces of cellular senescence. *J Cell Biol* 192(4):547–556.
2. Campisi J, d'Adda di Fagagna F (2007) Cellular senescence: When bad things happen to good cells. *Nat Rev Mol Cell Biol* 8(9):729–740.
3. Coppé JP, Desprez PY, Krtolica A, Campisi J (2010) The senescence-associated secretory phenotype: The dark side of tumor suppression. *Annu Rev Pathol* 5:99–118.
4. Krtolica A, Parrinello S, Lockett S, Desprez PY, Campisi J (2001) Senescent fibroblasts promote epithelial cell growth and tumorigenesis: A link between cancer and aging. *Proc Natl Acad Sci USA* 98(21):12072–12077.
5. Mu XC, Higgins PJ (1995) Differential growth state-dependent regulation of plasminogen activator inhibitor type-1 expression in senescent IMR-90 human diploid fibroblasts. *J Cell Physiol* 165(3):647–657.
6. Kuilman T, Peeper DS (2009) Senescence-messaging secretome: SMS-ing cellular stress. *Nat Rev Cancer* 9(2):81–94.
7. Dimri GP, et al. (1995) A biomarker that identifies senescent human cells in culture and in aging skin in vivo. *Proc Natl Acad Sci USA* 92(20):9363–9367.
8. Wahl GM, Carr AM (2001) The evolution of diverse biological responses to DNA damage: Insights from yeast and p53. *Nat Cell Biol* 3(12):E277–E286.
9. Herbig U, Jobling WA, Chen BP, Chen DJ, Sedivy JM (2004) Telomere shortening triggers senescence of human cells through a pathway involving ATM, p53, and p21 (CIP1), but not p16(INK4a). *Mol Cell* 14(4):501–513.
10. Serrano M, Lin AW, McCurrach ME, Beach D, Lowe SW (1997) Oncogenic ras provokes premature cell senescence associated with accumulation of p53 and p16INK4a. *Cell* 88(5):593–602.
11. Parrinello S, et al. (2003) Oxygen sensitivity severely limits the replicative lifespan of murine fibroblasts. *Nat Cell Biol* 5(8):741–747.
12. Baker DJ, et al. (2011) Clearance of p16Ink4a-positive senescent cells delays ageing-associated disorders. *Nature* 479(7372):232–236.
13. Kuro-o M, et al. (1997) Mutation of the mouse klotho gene leads to a syndrome resembling ageing. *Nature* 390(6655):45–51.
14. Baker DJ, et al. (2008) Opposing roles for p16Ink4a and p19Arf in senescence and ageing caused by BubR1 insufficiency. *Nat Cell Biol* 10(7):825–836.
15. Liu H, et al. (2007) Augmented Wnt signaling in a mammalian model of accelerated aging. *Science* 317(5839):803–806.
16. Doi S, et al. (2011) Klotho inhibits transforming growth factor-beta1 (TGF-beta1) signaling and suppresses renal fibrosis and cancer metastasis in mice. *J Biol Chem* 286(10):8655–8665.
17. Kurosu H, et al. (2005) Suppression of aging in mice by the hormone Klotho. *Science* 309(5742):1829–1833.
18. Takeshita K, et al. (2002) Increased expression of plasminogen activator inhibitor-1 with fibrin deposition in a murine model of aging, "Klotho" mouse. *Semin Thromb Hemost* 28(6):545–554.
19. Kortlever RM, Higgins PJ, Bernards R (2006) Plasminogen activator inhibitor-1 is a critical downstream target of p53 in the induction of replicative senescence. *Nat Cell Biol* 8(8):877–884.
20. Boe AE, et al. (2013) Plasminogen activator inhibitor-1 antagonist TM5441 attenuates Nω-nitro-L-arginine methyl ester-induced hypertension and vascular senescence. *Circulation* 128(21):2318–2324.
21. Morishita K, et al. (2001) The progression of aging in klotho mutant mice can be modified by dietary phosphorus and zinc. *J Nutr* 131(12):3182–3188.
22. Coviello-McLaughlin GM, Prowse KR (1997) Telomere length regulation during postnatal development and ageing in Mus spretus. *Nucleic Acids Res* 25(15):3051–3058.
23. Suga T, et al. (2000) Disruption of the klotho gene causes pulmonary emphysema in mice. Defect in maintenance of pulmonary integrity during postnatal life. *Am J Respir Cell Mol Biol* 22(1):26–33.
24. Voelkl J, et al. (2013) Spironolactone ameliorates PIT1-dependent vascular osteoinduction in klotho-hypomorphic mice. *J Clin Invest* 123(2):812–822.
25. Fischer SS, et al. (2010) Hyperaldosteronism in Klotho-deficient mice. *Am J Physiol Renal Physiol* 299(5):F1171–F1177.
26. Eren M, Painter CA, Atkinson JB, Declerck PJ, Vaughan DE (2002) Age-dependent spontaneous coronary arterial thrombosis in transgenic mice that express a stable form of human plasminogen activator inhibitor-1. *Circulation* 106(4):491–496.
27. Bernot D, et al. (2011) Plasminogen activator inhibitor 1 is an intracellular inhibitor of furin proprotein convertase. *J Cell Sci* 124(Pt 8):1224–1230.
28. Fukumoto S (2005) Post-translational modification of Fibroblast Growth Factor 23. *Ther Apher Dial* 9(4):319–322.
29. Thomas G (2002) Furin at the cutting edge: From protein traffic to embryogenesis and disease. *Nat Rev Mol Cell Biol* 3(10):753–766.
30. Tian S, Huang Q, Fang Y, Wu J (2011) FurinDB: A Database of 20-Residue Furin Cleavage Site Motifs, Substrates and Their Associated Drugs. *Int J Mol Sci* 12(2):1060–1065.
31. Razzaque MS (2009) The FGF23-Klotho axis: Endocrine regulation of phosphate homeostasis. *Nat Rev Endocrinol* 5(11):611–619.
32. Yamamoto M, et al. (2005) Regulation of oxidative stress by the anti-aging hormone klotho. *J Biol Chem* 280(45):38029–38034.
33. Hu MC, et al. (2011) Klotho deficiency causes vascular calcification in chronic kidney disease. *J Am Soc Nephrol* 22(1):124–136.
34. Ohnishi M, Nakatani T, Lanske B, Razzaque MS (2009) Reversal of mineral ion homeostasis and soft-tissue calcification of klotho knockout mice by deletion of vitamin D 1alpha-hydroxylase. *Kidney Int* 75(11):1166–1172.
35. Lim K, et al. (2012) Vascular Klotho deficiency potentiates the development of human artery calcification and mediates resistance to fibroblast growth factor 23. *Circulation* 125(18):2243–2255.
36. Brown NJ, et al. (2000) Aldosterone modulates plasminogen activator inhibitor-1 and glomerulosclerosis in vivo. *Kidney Int* 58(3):1219–1227.
37. Elzi DJ, et al. (2012) Plasminogen activator inhibitor 1—insulin-like growth factor binding protein 3 cascade regulates stress-induced senescence. *Proc Natl Acad Sci USA* 109(30):12052–12057.
38. Liu F, Wu S, Ren H, Gu J (2011) Klotho suppresses RIG-I-mediated senescence-associated inflammation. *Nat Cell Biol* 13(3):254–262.
39. López-Andrés N, et al. (2013) Absence of cardiotrophin 1 is associated with decreased age-dependent arterial stiffness and increased longevity in mice. *Hypertension* 61(1):120–129.
40. Peeper DS (2011) Ageing: Old cells under attack. *Nature* 479(7372):186–187.
41. Tashiro Y, et al. (2012) Inhibition of PAI-1 induces neutrophil-driven neoangiogenesis and promotes tissue regeneration via production of angiocrine factors in mice. *Blood* 119(26):6382–6393.
42. Izuhara Y, et al. (2008) Inhibition of plasminogen activator inhibitor-1: Its mechanism and effectiveness on coagulation and fibrosis. *Arterioscler Thromb Vasc Biol* 28(4):672–677.
43. Izuhara Y, et al. (2010) A novel inhibitor of plasminogen activator inhibitor-1 provides antithrombotic benefits devoid of bleeding effect in nonhuman primates. *J Cereb Blood Flow Metab* 30(5):904–912.
44. Miyata T, Yamaoka N, Kodama H, Murano K (2011) Inhibitor of plasminogen activator inhibitor-1. US Patent Appl 2,011,112,140 A1 (May 12, 2011).
45. Mutlu GM, et al. (2004) Upregulation of alveolar epithelial active Na+ transport is dependent on beta2-adrenergic receptor signaling. *Circ Res* 94(8):1091–1100.
46. Cawthon RM (2002) Telomere measurement by quantitative PCR. *Nucleic Acids Res* 30(10):e47.
47. Callicott RJ, Womack JE (2006) Real-time PCR assay for measurement of mouse telomeres. *Comp Med* 56(1):17–22.

本報告書は、厚生労働省の平成２６年度厚生労働科学研究委託事業(難治性疾患等克服研究事業(難治性疾患等実用化研究事業(難治性疾患実用化研究事業)))による委託業務として、国立大学法人東北大学が実施した平成２６年度「健康寿命の延伸、重症化遅延を目指した早老症治療薬の創出」の成果を取りまとめたものです。